NeuroImage 308 (2025) 121066

Contents lists available at ScienceDirect

NeuroImage

journal homepage: www.elsevier.com/locate/ynimg

Fiber length distribution characterizes the brain network maturation during early school-age

Yanlin Yu [a], Qing Cai [a,b,c,***], Longnian Lin [a,b,c,d,**], Chu-Chung Huang [a,b,c,*]

[a] Shanghai Key Laboratory of Brain Functional Genomics (Ministry of Education), Institute of Brain and Education Innovation, School of Psychology and Cognitive Science, East China Normal University, Shanghai, China
[b] Shanghai Center for Brain Science and Brain-Inspired Technology, Shanghai, China
[c] NYU-ECNU Institute of Brain and Cognitive Science, New York University Shanghai, Shanghai, China
[d] School of Life Science Department, East China Normal University, Shanghai 200062, China

ARTICLE INFO

Keywords:
Early-school age
Longitudinal study
Fiber length distribution
Network topology
White matter development

ABSTRACT

Environmental and social changes during early school age have a profound impact on brain development. However, it remains unclear how the brains of typically-developing children adjust white matter to optimize network topology during this period. This study proposes fiber length distribution as a novel nodal metric to capture the continuous maturation of brain network. We acquired dMRI data from N = 30 typically developing children in their first year of primary school and a one-year follow-up. We assessed the longitudinal changes in fiber length distribution, characterized by the median length of connected fibers for each brain region. The length median was positively correlated with degree and betweenness centrality, while negatively correlated with clustering coefficient and local efficiency. From ages 7 to 8, we observed significant decreases in length median in the temporal, superior parietal, anterior cingulate, and medial prefrontal cortices, accompanied by a reduction in long-range connections and an increase in short-range connections. Meta-analytic decoding revealed that the widespread decrease in length median occurred in regions responsible for sensory processing, whereas a more localized increase in length median was observed in regions involved in memory and cognitive control. Finally, simulation tests on healthy adults further supported that the decrease in long-range connections and increase in short-range connections contributed to enhanced network segregation and integration, respectively. Our results suggest that the dual process of short- and long-range fiber changes reflects a cost-efficient strategy for optimizing network organization during this critical developmental stage.

1. Introduction

Early school age is a critical period during which substantial transformations in children's social and learning environments, alongside the refinement of brain networks, play a pivotal role in cognitive development (Gooch et al., 2016; Nagy et al., 2004; Strong et al., 2005). As the foundational architecture for brain network formation, white matter (WM) structure shows prolonged development from the mid-gestation through adolescence, marked by ongoing processes of myelination, synaptic proliferation, and pruning (Dubois et al., 2014; Krogsrud et al., 2016; Peters et al., 2014; Yu et al., 2020). These processes gradually enhance the efficiency of brain network communication (Baum et al., 2017; H. Huang et al., 2015; Zhao et al., 2019). Given that the brain is spatially constrained, the topological maturation process must balance the costs of connections, which are closely related to fiber length (Milisav and Misic, 2023). However, how brain regions adjust the balance of long- and short-range connections to promote network maturation and influence cognitive development remains unclear.

* Corresponding authors at: Shanghai Key Laboratory of Brain Functional Genomics (Ministry of Education), Institute of Brain and Education Innovation, School of Psychology and Cognitive Science, East China Normal University, Shanghai, China
** Corresponding authors at: School of Life Science Department, East China Normal University, 3663 N. Zhongshan Road, Shanghai 200062, China.
*** Corresponding authors at: Shanghai Key Laboratory of Brain Functional Genomics (Ministry of Education), Institute of Brain and Education Innovation, School of Psychology and Cognitive Science, East China Normal University, Shanghai, China.
E-mail addresses: qcai@psy.ecnu.edu.cn (Q. Cai), lnlin@brain.ecnu.edu.cn (L. Lin), czhuang@psy.ecnu.edu.cn (C.-C. Huang).

https://doi.org/10.1016/j.neuroimage.2025.121066
Received 24 September 2024; Received in revised form 28 December 2024; Accepted 28 January 2025
Available online 28 January 2025

In studies of brain structural development, diffusion magnetic resonance imaging (dMRI) has been widely used as a non-invasive technique to examine WM structure and its topology (Lebel et al., 2019; Yu et al., 2020). Researchers have shown that WM connectivity strengthens with development and cognitive maturation (Sherman et al., 2014) with tractography-based connectome analyses highlighting the pattern of network topological change during this stage (Dubois et al., 2021; Feng et al., 2023; Zhao et al., 2015). During the development process, brain structural networks become increasingly segregated and integrated, gradually resembling adult brains (Zhao et al., 2015). This process is driven by enhanced within-module connectivity (Baum et al., 2017; Puxeddu et al., 2020) and the shifting of network hubs from primary cortical areas in early childhood to association areas in later childhood (Baker et al., 2015; Baum et al., 2017; Oldham et al., 2022; Oldham and Fornito, 2019; Puxeddu et al., 2020). These differential changes in structural connectivity contribute to the optimization of hierarchical brain organization (Menon, 2013).

However, how long- and short-range interregional connections change during development to facilitate network segregation and hierarchy remains elusive. Two crucial factors underscore the importance of incorporating fiber length into developmental network studies: (i) short-range connections are observed later myelination until the third decade of life compared to longer connections (Lebel et al., 2012; Lebel and Beaulieu, 2011; Ouyang et al., 2017; Oyefiade et al., 2018); and (ii) primary networks have relatively short-range connections, while transmodal networks possess longer-range fibers (Sepulcre et al., 2010). Recent research supports that the fiber length distribution within brain regions can differentiate the complexity of functional networks (Bajada et al., 2019). Therefore, differences in maturation periods and functions between short- and long-range connections suggest that the length properties of interregional connections may change with age, reflecting alterations in the hierarchical positioning of these regions within an anatomically constrained brain network.

In this study, we first propose regional fiber length distribution as a novel nodal metric to describe how longitudinal alterations in WM arrangement facilitate topology maturation in early school-age children. Specifically, we associated the regional fiber length distribution with topological properties and studied its longitudinal changes from ages 7 to 8. We conducted a meta-analytic decoding to investigate its functional meaning and performed a simulation test on healthy adults to determine the effect of connection distances on network topological properties. We hypothesize that longitudinal changes in fiber length distribution reveal how brain regions adjust their topological properties to support higher-order cognitive development in early school-age children, offering a novel perspective to explain how the brain becomes structurally more efficient.

2. Methods and materials

2.1. Participants

2.1.1. Children dataset

Among 317 participants undergoing MRI scans from the East China Normal University Study of Brain and Intellectual Developmental Mechanisms in Children and Adolescents Project, a total of 70 children without neurological disorders or intellectual disabilities were initially recruited, This study included 30 children (18 females and 12 males) who completed both T1-weighted and diffusion MRI imaging during their first grade in primary school (7.5 ± 0.3 yr) and at a one-year follow-up (8.6 ± 0.3 yr) (Table 1). This longitudinal cohort study was approved by the East China Normal University Ethics Committee, with written informed consent obtained from all participants and their parents.

2.1.2. Adult dataset

The adult dataset was used for a simulation test to investigate the spatial effect on topology. The dataset comprised 41 healthy (24 females and 17 males, 20.3 ± 1.6 yr) adults without physiological or psychological issues, also approved by the East China Normal University Ethics Committee.

Table 1
Demographic Characteristics of the Participants.

Characteristics	Adults (n = 41)	Children (n = 30)		
		Baseline mean (SD)	Follow-up mean(SD)	p-value
Sex, men/women	17/24	12/18		
Age (years)	20.3 (1.6)	7.5 (0.3)	8.6 (0.3)	
Education (years)	12.8 (1.6)	1 (0)	2 (0)	
Kindergarten age (years)	–	3.7 (0.7)	–	
SWM	–	5.3 (1.2)	5.3 (1.1)	0.895
ICV	1.45 (0.12) × 10^6	1.36 (0.13) × 10^6	1.38 (0.12)	0.068
WMV	5.60 (0.56) × 10^5	4.84 (0.53) × 10^5	4.95 (0.52)	0.008*
GMV	6.14 (0.55) × 10^5	6.73 (0.65) × 10^5	6.75 (0.61)	0.801

Abbreviations: SWM, Spatial Working Memory; ICV, Intracranial Volume; WMV, White Matter Volume; GMV, Gray Matter Volume. Analysis performed with paired t-test between baseline and follow-up in children dataset. * p-value < 0.05.

2.2. MRI acquisition

2.2.1. Children dataset

High-resolution T1-weighted (T1 w) images were acquired using a (TR/TE = 2300/2.5 ms, flip angle = 8°, FOV = 224 mm, matrix size: 224 × 224, 192 sagittal slices, voxel size = 1 mm isotropic). The multi-shell diffusion-weighted images (DWIs) were acquired using a single shot spin-echo planar imaging sequence (TR/TE = 3200/75 ms, matrix size = 128 × 128, voxel size = 2 mm isotropic, multiband factor = 3, phase encoding: anterior to posterior) with b-values of 1000 s/mm2 (64 diffusion directions), 2000 s/mm2 (64 diffusion directions) and a b0 image. A reverse phase-encoded (posterior to anterior) image was acquired to correct magnetic susceptibility-induced phase encoding direction artifacts.

2.2.2. Adult dataset

High-resolution T1-weighted (T1 w) images were acquired using a (TR/TE = 2500/2.22 ms, flip angle = 8°, FOV = 224 mm, matrix size: 208 × 300, 192 sagittal slices, voxel size=0.8 mm isotropic). The multi-shell diffusion-weighted images (DWIs) were acquired using a single shot spin-echo planar imaging sequence (TR/TE = 6600/73 ms, matrix size = 140 × 140, voxel size = 1.5 mm isotropic, multiband factor = 3, phase encoding: anterior to posterior) with b-values of 1000 s/mm^2 (30 diffusion directions), 3000 s/mm^2 (60 diffusion directions) and 9 b0 images interleaved. A reverse phase-encoded (posterior to anterior) image was acquired to correct magnetic susceptibility-induced phase encoding direction artifacts.

2.3. Data preprocessing

We used the Integrated Diffusion Image Operator (iDIO) pipeline (https://github.com/iDIO4dMRI/iDIO) for T1 w and DWI image (Hsu et al., 2023), preprocessing steps including (1) denoising (Veraart et al., 2016), (2) Gibbs ringing artifacts removal,(Kellner et al., 2016) (3) signal drifting correction (Vos et al., 2017), (4) correction for eddy current induced distortion and head movements (S. M. Smith et al., 2004), (5) susceptibility distortion correction (S. M. Smith et al., 2004), (6) B1 field inhomogeneity correction (Tustison et al., 2010). A Multi-Shell Multi-Tissue Constrained Spherical Deconvolution (MSMT

CSD) model was performed to estimate WM fiber orientation distribution (FOD) (Dhollander et al., 2016; Jeurissen et al., 2014). All the tissue generated was applied multi-tissue informed log-domain intensity normalization (Raffelt et al., 2017).

T1 w image preprocessing includes Gibbs-ringing artifact removal, B1 field inhomogeneity bias correction, and a brain mask generated with skull-stripped using the antsBrainExtraction function (Avants et al., 2009). A five-tissue-type (5tt) segmentation image was generated based on the T1-weighted image and then transformed to DWI space to improve the biological accuracy of tractography reconstruction (Patenaude et al., 2011; R. E. Smith et al., 2012; S. M. Smith, 2002; S. M. Smith et al., 2004).

2.4. Tractography

2.4.1. Children dataset

Due to the fiber length may be highly related to brain size, we built a longitudinal FOD template to control the effects of brain size and subtle variation between longitudinal individuals (Genc et al., 2018). For each participant, the timepoint 1 and timepoint 2 FOD maps were first transformed rigidly to their midway space and averaged to generate an intra-subject FOD template. All 30 intra-subject FOD templates were used to generate the unbiased longitudinal group template. For each participant, the FOD map was registered to the group FOD template by composing the linear and nonlinear transformations. The 5tt image was then registered to the template space.

The anatomically constrained tractography (ACT) was reconstructed using the iFOD2 (second-order integration) with a dynamic seeding algorithm where 20 million streamlines were generated (maximum tract length = 250 mm, minimal tract length = 5 mm, FOD amplitude = 0.05, curve angle = 45°) (R. E. Smith et al., 2015a; Tournier et al., 2010) based on the FOD in each participant's registered-template. The registered 5tt image was used as prior biological information to ensure the streamlines terminated at the GM-WM interface.(R. E. Smith et al., 2012) To improve the estimation of structural connection density, the spherical-deconvolution informed filtering of tractography (SIFT) was then applied, remaining 2 million streamlines per participant (R. E. Smith et al., 2013).

2.4.2. Adult dataset

The tractography parameters are identical to those for the children dataset.

The effect of brain size was not controlled in the simulation tests. The probabilistic tractography was reconstructed based on the native FOD, with 20 million streamlines generated and then filtered, leaving 2 million remaining.

2.5. Connectome reconstruction

Structural connectomes were generated based on the HCPex atlas (containing 360 cortical regions and 66 subcortical regions) (Hagmann et al., 2008; C.-C. Huang et al., 2022; R. E. Smith et al., 2015b). The atlas was transformed into native space for adults (Fig. 1A) and longitudinal template space for children (Fig. 1C) respectively (details in Method S1). The number of streamlines between pairs of brain regions were measured, producing two 360 × 360 matrices for each individual per timepoint. By calculating the average length of streamlines in pairs of brain regions, we calculated the average length of streamlines assigned to each edge, generating the length connectome for each participant. To ensure the edge stability of the connectome, we applied a population-based connectome mask to each participant's length connectome (Figure 1D; Method S2).

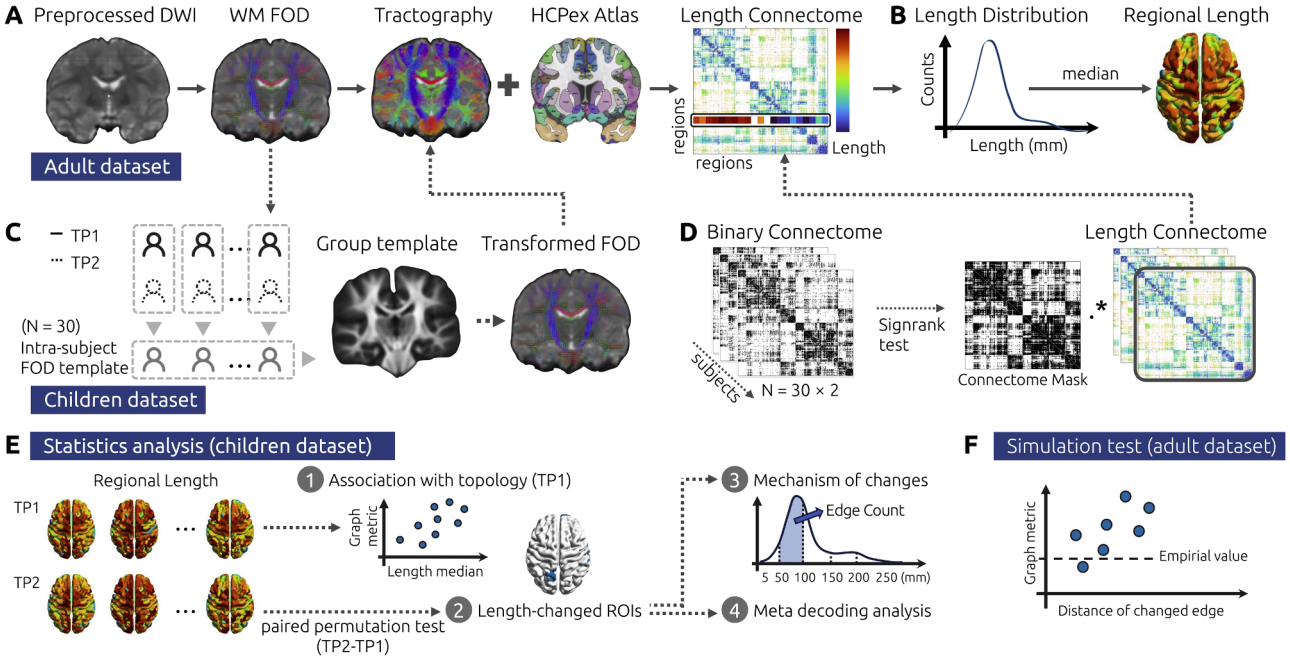

Fig. 1. Analysis workflow for the regional length. A, The workflow of Length Connectome reconstruction for both datasets. B, The fiber length distribution for each brain region is characterized by the nonzero value of each row/column of length connectome. The regional length is the median for fiber length distribution for its non-normality. C, Longitudinal group FOD template generation for children dataset. For each participant, the timepoint 1 and timepoint 2 FOD maps were first transformed rigidly to their midway space and averaged to generate an intra-subject FOD template. All 30 intra-subject FOD templates generated by averaging were used to generate the unbiased longitudinal group template. Each participant's FOD was linearly transformed to their intra-subject template and then nonlinearly transformed to the group FOD template. The tractography was generated based on the transformed FOD and then the tractography-based connectome was reconstructed using the HCPex atlas. D, Connectome reconstruction. Each edge within the binary connectome performed the two-sided signed rank test to generate the connectome mask. For each length connectome was applied the connectome mask to retain the significantly-existed edges in this population. E, The statistics analysis for comparison of the regional length map (TP2-TP1). F, The simulation test was performed on an adult dataset to further investigate the geometric-related effect on the topological features.

2.6. Regional fiber length

For each brain region, the length of connectome rows was extracted to build the fiber length distribution for 360 cortical brain regions. Given the length distribution may be skewed towards short-range connections, the regional length was characterized by the nonzeros median for fiber length distribution of brain regions (Fig. 1B).

2.7. Topological properties

Graph theoretical measures for the binary structural connectome (360 cortical regions) of children were calculated using the Brain Connectivity Toolbox (https://sites.google.com/site/bctnet/measures/list) (Rubinov and Sporns, 2010). The measures included the global metric: global efficiency, and the nodal metrics: degree, betweenness centrality (representing integration), clustering coefficient, and local efficiency (representing segregation).

2.8. Association between topology and regional length

To investigate the topological meaning of the regional length, we examined the Pearson correlation between length median and nodal graph metrics (averaged over subjects) for the children dataset at baseline. We performed the null models to determine whether such associations exist if the brain is not a spatial embedding system (Method S3).

2.9. Longitudinal changes in length median and its underlying mechanism

The differences in the length median for each brain region between two time points were assessed using a paired two-sample permutation test (detailed in https://statlab.github.io/permute/user/one-sample.html). We found the length-changed regions of interest (length-changed ROIs) with significant differences during development (1000 permutations, $p < 0.01$). To investigate how the region's connecting edges change leading to alteration in its fiber length distribution, we stratified the edges within the length connectome into five length ranges: 5–50 mm, 50–100 mm, 100–150 mm, 150–200 mm, and 200–250 mm, then compared the count of node's connecting edges falling within each length range using paired *t*-test.

2.10. Cognitive functions decoding

We conducted the meta-analytic decoding from the Neurosynth database (www.neurosynth.org) (Yarkoni et al., 2011) to identify the cognitive functions of length-changed ROIs. To further assess the association between cognitive functions and spatial patterns of age-related change in the regional length, we assigned 360 brain regions into 2 subsets according to the t-value (unthresholded positive and negative t-values) obtained from the comparison of length median and then associated the absolute t-values maps of 2 subsets with 24 Neurosynth topic terms covering a wide range of functions (Margulies et al., 2016; Paquola et al., 2019).

2.11. Simulated networks

We performed the simulation tests on healthy adults to demonstrate how changing connections at different Euclidean distance (ED) would affect the topological properties for adult dataset (Fig. 2A). Based on the empirical connectivity matrix, only one connecting edge was either removed or added respectively at a time to regenerate the simulated network. We then calculated the Pearson correlation between the ED of the changed edge and corresponding global and nodal graph metrics derived from the simulated networks to investigate the geometry-related effect on network topology (Fig. 2A). Considering that primary and hetero-modal association cortices may play different roles in the network, we selected L_V1 (primary visual cortex) and L_46 (dorsolateral prefrontal cortex, dlPFC) as representative brain regions due to their distinctions in both anatomical position and functional hierarchy.

In addition, to consider the effect of subcortical regions, the length median and graph metrics were calculated for connectomes with 426 brain regions (including 66 subcortical areas), and all analyses were repeated to validate the stability of length median metric (see details in supplementary material).

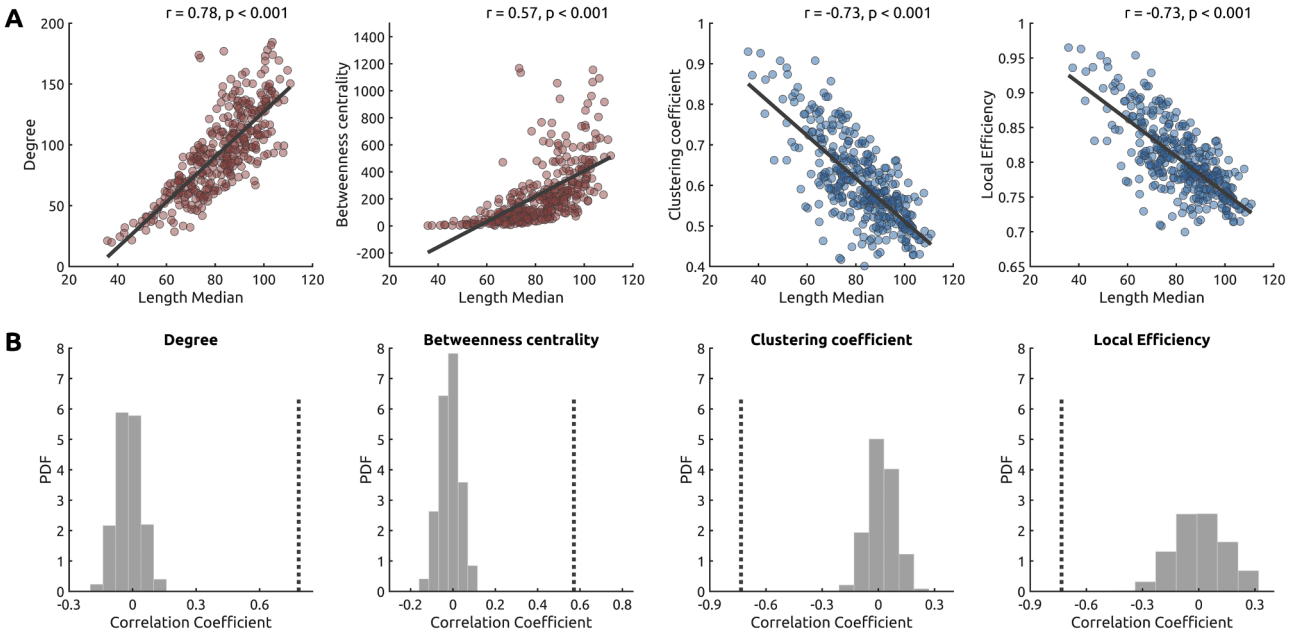

Fig. 2. The association with topological characteristics of the network. A, The correlation between regional length and graph metrics at baseline. B, The histograms represent the Pearson correlation coefficients across regional length and graph metrics of the null model derived from 1000 permutations. The dashed lines represent the empirical Pearson correlation coefficients.

3. Results

3.1. Longitudinal changes in brain volumes

Intracranial volume (ICV) and gray matter volume (GMV) showed no significant differences between the two time points, while white matter volume (WMV) increased significantly at the second time point ($t = 2.82$, $p = 0.008$) (Table 1). These results indicated an increase in white matter volume during the transition from 7 to 8 years of age, while gray matter volume remained unchanged.

3.2. Association between regional length median and graph metrics

At baseline, the regional length was positively correlated with graph-theoretical integration metrics, including degree ($r = 0.78$, $p < 0.001$), and betweenness centrality ($r = 0.57$, $p < 0.001$) but negatively correlated with segregation metrics including the clustering coefficient ($r = -0.73$, $p < 0.001$) and local efficiency ($r = -0.73$, $p < 0.001$) (Fig. 2A). The correlation between the region's length median and graph metrics remains significant when comparing correlation to 1000 null models (Fig. 2B). The associations between length median and topology are stable across different sparsities and graph metrics derived from the weighted connectome (Figure S1, Figure S3, and Figure S4). Additionally, these graph metrics exhibited no significant associations with brain volume.

3.3. Longitudinal changes in regional length during early school age and its underlying mechanism

By comparing the length median between two time points in early school-age children, we found that the length median of most brain regions decreased over the one-year interval. Brain regions with a significantly decreased length median (termed length-decreased ROIs) included L_TF, L_PHA1, L_TE1 m, L_7Am, L_7PL, L_VIP, L_25, L_a24, R_PBelt, and R_10d. Only R_FOP1 showed a significant increase in length median (termed length-increased ROI) over the one-year interval (Figure 3A; Table 2). One-sample *t*-tests on the t-values of brain regions within cortical divisions showed that the cortex with significant reductions in fiber length distribution were located in the early auditory, auditory association, lateral temporal, superior parietal, anterior cingulate, and medial prefrontal cortex (Fig. 3B). The effects of applying and not applying the connectome mask on the changes of regional length median were evaluated and shown in the supplementary results (Result S2; Figure S2).

To further explain the mechanisms underlying these changes, we analyzed the length distribution by comparing the counts of edges across different length ranges. We found a general pattern that the count of short-range connections increased in most brain regions regardless of the change direction of length median. However, the count of longer-range connections decreased in length-decreased regions, and conversely increased in length-increased regions. (Figure 3C; Figure S6).

3.4. Meta-analytic functional decoding

The meta-analysis showed that the length-changed ROIs are most related to autobiographical memory (Fig. 4A). Furthermore, the brain regions that exhibited increasing fiber length distribution are more related to integrative functions, such as "episodic memory", "cognitive control" and "inhibition". While the brain regions showed decreasing fiber length distribution are more related to sensory processes, such as "auditory", "multisensory", "action" and "visuospatial". Critically, some cognitive functions are associated with both subsets, such as "social cognition", "emotion", "autobiographical memory", "language", "reading", and "semantics" (Fig. 4B).

The longitudinal results remained unchanged when subcortical regions were included in the connectome (see details in supplementary results, Figure S8, Figure S9, Figure S10 and Figure S11; Table S1).

3.5. Effects of edge length on network topological properties

To demonstrate the dynamics of topological alterations affected by changing connection in different distance, we calculated the graph metrics for two selected brain regions (L_46 and L_V1) with only one connection removed or added then correlated the changed connection length with corresponding graph metrics. For both brain regions, ED of added edge is positively correlated with network integration (global efficiency and betweenness centrality), while negatively correlated with segregation (clustering coefficient and local efficiency). Conversely, the ED of the removed edge is positively correlated with network segregation and negatively correlated with integration (Fig. 5B, Figure S12), indicating that removing longer range connection leads to higher segregation and lower integration, while adding longer range connection leads to higher integration and lower segregation. Simulations conducted on other brain regions in the adult dataset also showed similar patterns (Figure S11).

4. Discussion

In this study, we identified longitudinal changes in fiber length median among early school-age children from age 7 to 8 years. We found a general decrease in length median in the fronto-parietal and medial temporal areas, along with increased short-range and decreased long-range fiber connections. Meta-analytic functional decoding suggested that reduced length median in brain regions is linked to sensory processing, while increased length median in brain regions related with memory and cognitive control. Simulation tests in healthy adults indicated these alterations reflect a balance between network segregation and integration, highlighting the developmental maturation of brain

Table 2
Alterations in the regional length.

ID	Region	RegionLongName	Cortical Division	t-value	p-value
Length-decreased ROIs					
84	L_TF	Area_TF	Medial_Temporal	−3.849	0.002
85	L_PHA1	ParaHippocampal_Area_1	Medial_Temporal	−3.109	0.004
90	L_TE1m	Area_TE1_Middle	Lateral_Temporal	−2.971	0.006
102	L_7Am	Medial_Area_7A	Superior_Parietal	−3.487	0.004
104	L_7PL	Lateral_Area_7P	Superior_Parietal	−2.96	0.01
110	L_VIP	Ventral_IntraParietal_Complex	Superior_Parietal	−2.483	0.006
136	L_25	Area_25	Anterior_Cingulate_and_Medial_Prefrontal	−3.166	0.004
140	L_a24	Area_a24	Anterior_Cingulate_and_Medial_Prefrontal	−2.942	0.002
237	R_PBelt	ParaBelt_Complex	Early_Auditory	−3.282	0.002
330	R_10d	Area_10d	Orbital_and_Polar_Frontal	−3.285	0.01
Length-increased ROIs					
229	R_FOP1	Frontal_Opercular_Area_1	Posterior_Opercular	2.781	0.01

1000 permutations, $p < 0.01$.

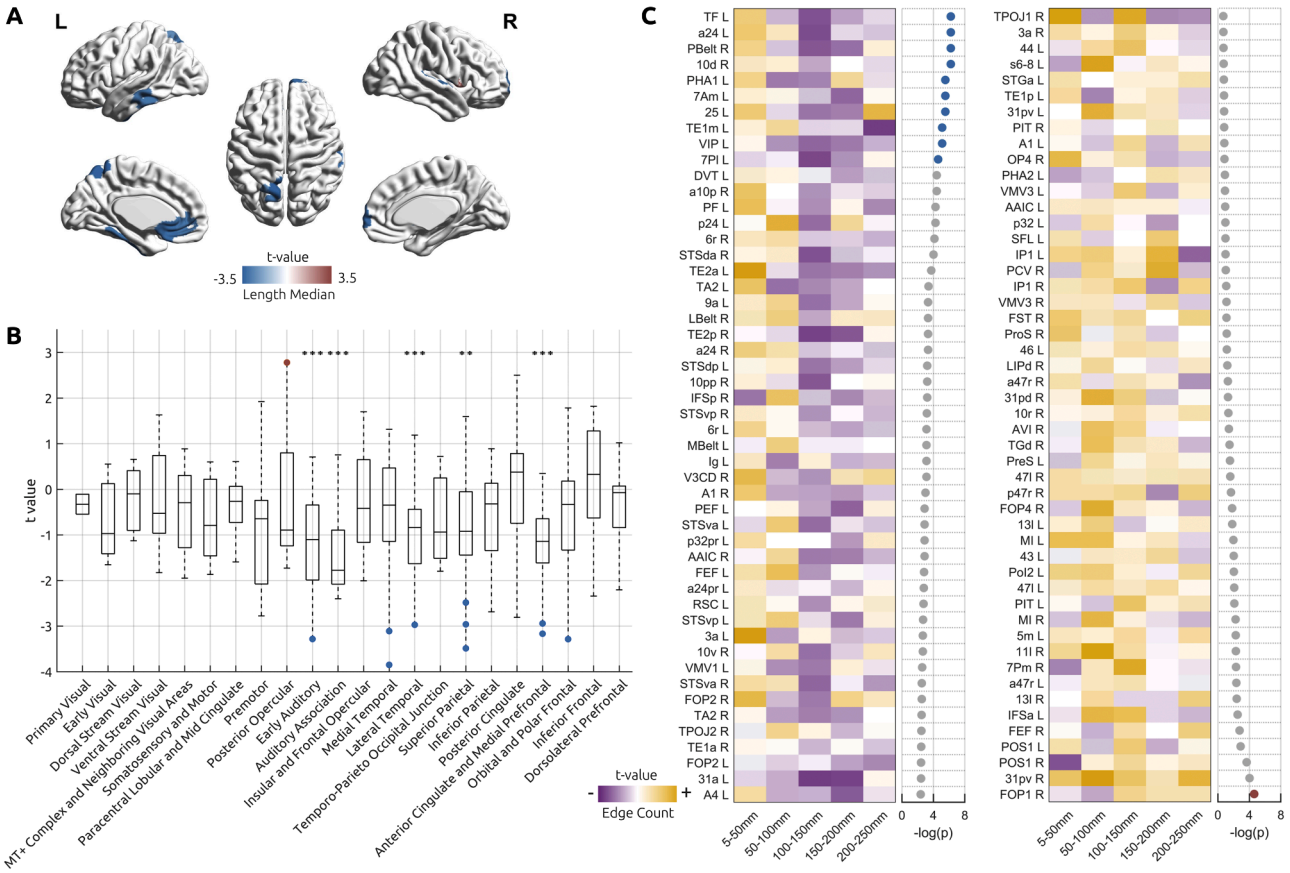

Fig. 3. Developmental changes in regional length. A, The brain regions with significant longitudinal changes (1000 permutations, $p < 0.01$). B, The spatial pattern of altered fiber length distribution of brain regions ordered by their belonging cortex based on the HCPex atlas. The blue dots represent the regions with significantly decreased length distribution, while the red dots represent the regions with significantly increased length distribution. One-sample *t*-tests were then performed for the t values of regions within the belonging cortex. The cortex that survived the FDR correction is denoted by asterisks. C, The matrices show the comparison of the count of edges at two-time points in different length ranges. Yellow represents an increase in the number of edges and purple represents a decrease. The columns of the matrix represent connections of different length ranges projected from brain regions. The rows of the matrix are the brain regions ordered according to the p values obtained from the comparison of length median at two-time points. The log-transformed p-value for each brain region is shown at the corresponding position of the right panel. Gray dots represent brain regions with insignificant differences in length median. The matrices list only the top 100 most significantly-changed cortical regions (50 increasing and 50 decreasing). The complete list can be found in the Figure S5.

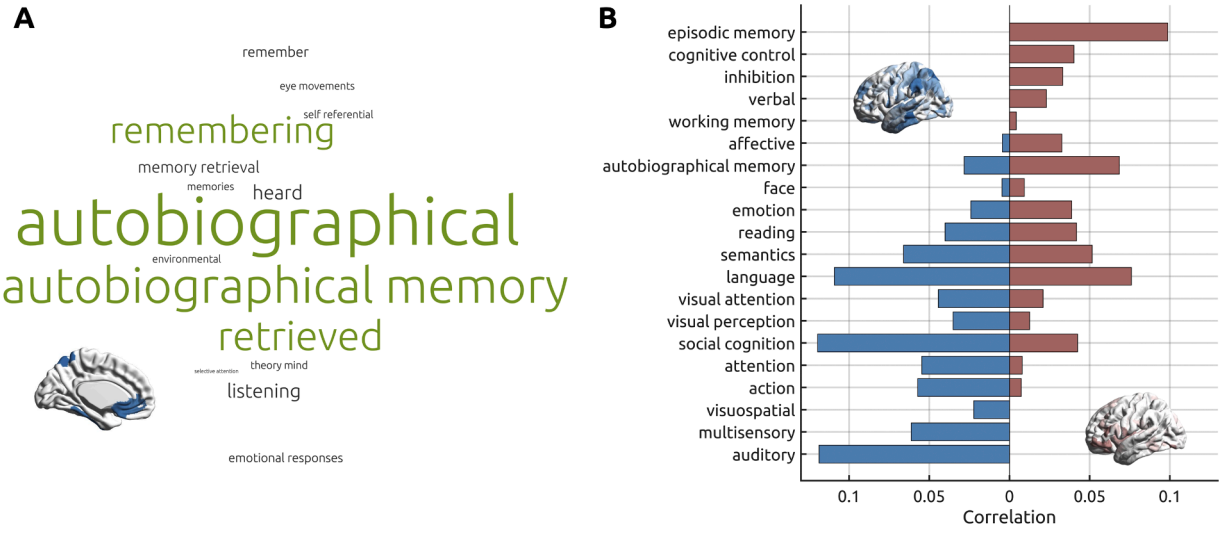

Fig. 4. The mechanism and Neurosynth topic representation of alterations in regional length. A, NeuroSynth decoding for the significantly changed regions in fiber length distribution (ROIs). Topic terms with large size represent higher probability. B, NeuroSynth continuous decoding for brain regions with positive t-value (age-related increase in regional length, red) and negative t-value (age-related decrease in regional length, blue) respectively using 24 topic terms. The rows (cognitive terms) were organized based on the difference in correlations from continuous decoding of absolute positive and negative t-values to, calculated as $\frac{r_{pos}-r_{neg}}{r_{pos}+r_{neg}}$.

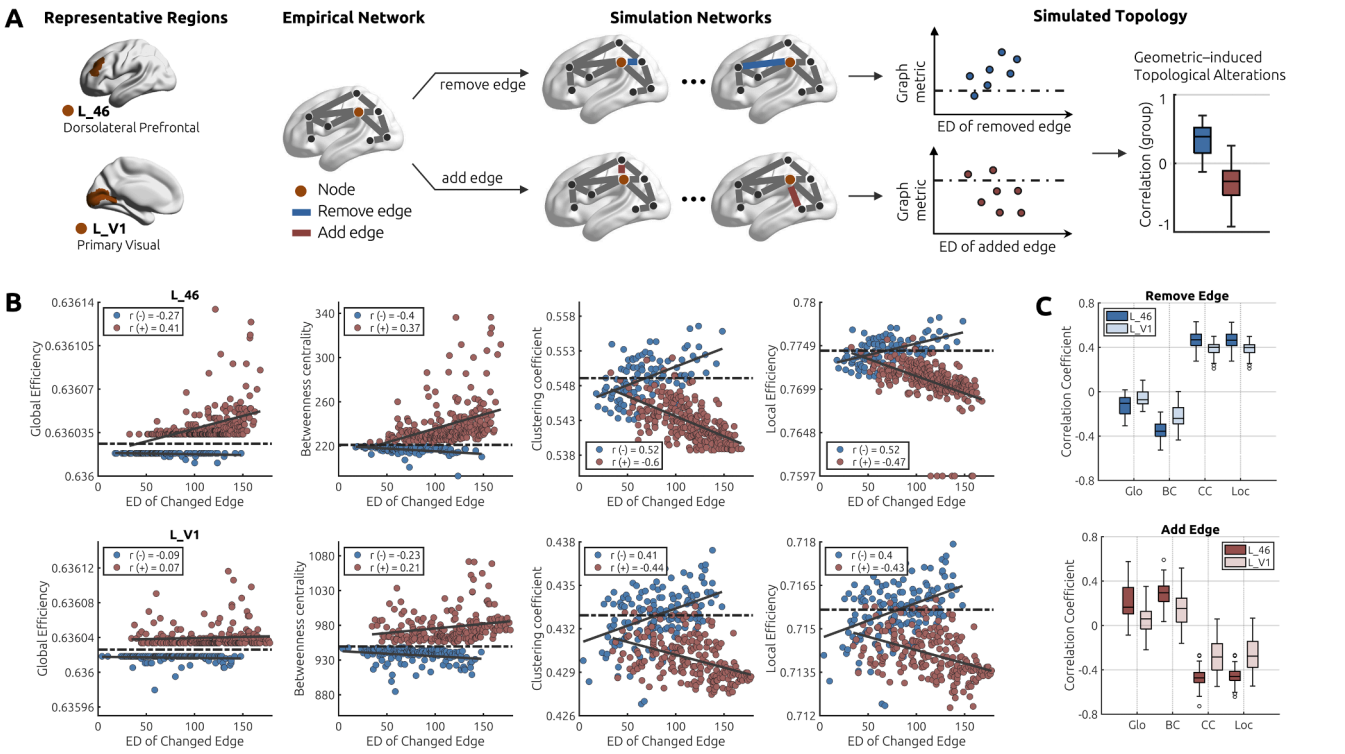

Fig. 5. Simulation test on the adult dataset. A, The workflow for the simulation test. L_46 (located in the dorsolateral prefrontal cortex) and L_V1 (located in the primary visual cortex) were selected as representative brain regions for the simulation test. For a specific brain region, only one connecting edge was removed (blue) or added (red) for each simulation. Then the Pearson correlations between the Euclidean distance of removed/added edge and the corresponding graph metrics were calculated. The dashed lines represent the empirical graph metrics. B, The Pearson correlations between the Euclidean distance of changed edge and global/nodal graph metrics for an arbitrarily chosen participant in the adult dataset. C, The boxplot of the correlation coefficients in the adult dataset. A higher absolute value of the correlation coefficient represents a larger geometric effect on the topological features.

structures in early school-age children from a network topological perspective.

The proposed regional length, characterized by the median of inter-regional fiber length distribution, measures a brain region's capability to connect distal areas and may serve as an indicator of network integration or segregation (Bajada et al., 2019). Longitudinal observations further revealed a widespread decrease in fiber length median, particularly in the superior parietal, medial prefrontal cortices, anterior cingulate, and temporal lobe. Notably, regions within the fronto-parietal network (FPN), including VIP, 7PL, 7Am in the left superior parietal lobe, and a24, 25, 10d in the left prefrontal cortex, showed significant reductions in length median, indicating the critical role of FPN in cognitive development, such as executive function, reasoning, and intelligence (DeSerisy et al., 2021; Dumontheil et al., 2010; Wang et al., 2020). Research suggests that FPN become more segregated during development, associated with improved executive function (Parlatini et al., 2017; Wang et al., 2020). The anterior cingulate and medial prefrontal cortices, involved in task control, also showed increased segregation with age (Fair et al., 2007). Moreover, enhanced segregation was observed in the lateral temporal cortex during early development (Cao et al., 2017), supported by our findings of decreased length median in TE1 m and TF regions. The right frontal-opercular (r-FOP1) showed an increase in length median during this stage, potentially regulating posterior brain activity for response selection (Higo et al., 2011), while the integration of the cingulo-opercular network, associated with improved inhibitory control, also increased with age (Marek et al., 2015). These findings align with previous studies using structural (Baum et al., 2017; Puxeddu et al., 2020; Zhao et al., 2015) or functional connectome analyses (Tooley et al., 2022; Wu et al., 2013), suggesting ongoing optimization of brain topological organization, particularly in FPN regions.

We found that a reduction in long-range connections likely contributes to the changes in median fiber length observed in this stage of development. This reduction may result from axon pruning – a process that occurs from infancy to early adulthood – where unnecessary neural connections are eliminated through cell death (Liang et al., 2022) or small-scale synaptic reorganization, leading to a more efficient brain network (Low and Cheng, 2006). This provides evidence for the process of network reconfigurations during the early school age (Dong et al., 2021; Park et al., 2022; Stikov et al., 2011; Xia et al., 2022). An intriguing finding from our simulation test was that removing long-range connections increases segregation but does not significantly affect integration. This may be explained by percolation theory, which suggests that while synaptic pruning reduces some connections, the overall network maintains its efficiency because key connections are preserved (Razban et al., 2023). Combined with our findings of increasing white matter volume with age, we speculate that regions in FPN and lateral temporal lobes removed excess long-range connections to make space for further myelination of newly developed short- or long-range WM (Stikov et al., 2011). Conversely, fewer brain regions exhibit an increasing length median, suggesting that enhanced segregation outweighs integration at this stage.

Moreover, an age-related increase in short-range connections (5–50 mm) was found in most brain regions, aligning with previous studies (Ouyang et al., 2017). Our simulation tests indicate that adding short-range connections contributes to enhance network integration instead of increasing the clustering of nearby brain regions. Hence, we speculate that increasing short-range connections may represent a cost-effective strategy for enhancing integration, while removing short connections results in a decline in segregation, highlighting the crucial role of short-range connections in supporting network hierarchy. The simulation results in early-school-age children, consistent with findings

in adult dataset (Figure S12), further underscore the robustness of this finding across developmental stages. Abnormal pruning of short-range connection may reduce modularity and lead to mental illnesses (Alexander-Bloch et al., 2013), which was rarely observed in typically-developing children's brains. The simulation provides a dynamic representation of geometry-related topological variations, offering insights into underlying mechanisms that cannot be fully captured by snapshots at specific time points. Other regions were also simulated, demonstrating similar geometry-related effect on topology: removing longer range connection leads to higher segregation and lower integration, while adding longer range connection leads to higher integration and lower segregation (Figure S11). The consistent patterns observed in our simulations strongly support the rationale for using the length median as a nodal metric to characterize network topology.

One possible explanation for region-specific alterations in fiber length distribution is the economic trade-off principle, suggesting the brain must balance wiring cost and topological value as a spatial embedding system (Assaf et al., 2020; Bullmore and Sporns, 2012; Horvát et al., 2016; Sporns et al., 2007; Sporns and Honey, 2006; Thiebaut de Schotten and Forkel, 2022). Due to anatomical constraints, forming complex topology requires integrating local modules and distant areas through limited but well-arranged WM connections (Horvát et al., 2016; Thiebaut de Schotten and Forkel, 2022). Hub regions also exhibit more long-range connections with remote areas (Sporns et al., 2007), exemplified by the default-mode network (DMN), which shows the greatest geodesic distance from sensory/motor regions, underlining its role in integrating multisensory perception (Margulies et al., 2016; Smallwood et al., 2021). Despite higher wiring costs, longer connections are believed to act as shortcuts, enhancing communication efficiency by reducing path length (Bassett and Bullmore, 2017; Sporns and Zwi, 2004). Long-range connections link regions with dissimilar micro-architectures (Bazinet et al., 2023), improving system dynamics (Betzel and Bassett, 2018; Pang et al., 2023). Therefore, the communication range of a brain region may reflect its necessity for information transfer (Bullmore and Sporns, 2012; Sporns et al., 2007), particularly pronounced in the DMN and FPN-related regions. Based on our findings and previous research, we propose that the most effective strategy to optimize network efficiency within the existing children's brain network is to increase short-range connections while pruning long-range connections. This dual adjustment seems crucial for enhancing both segregation and integration, which is essential for cognitive development and the brain's structural adaptation during this critical stage (Low and Cheng, 2006; Ouyang et al., 2017).

The meta-analytic decoding results showed that brain regions with significant changes in fiber length distributions are primarily linked to autobiographical memory, which typically develops during the first decade of life (Bauer, 2015). Further analyses revealed that regions with decreased fiber length are more associated with the development of auditory and multi-sensory functions. This finding suggests that areas responsible for sensory functions are still maturing at this stage, and their increasing segregation from other areas within the network may benefit to overall network communication (Cassady et al., 2020; Rankin and Rinzel, 2019; Snyder and Alain, 2007). In contrast, regions with increasing fiber length median are linked to memory functions, implying that the development of autobiographical and episodic memory may depend on integrating multiple distant brain regions (Geib et al., 2017; Westphal et al., 2017). Overall, these meta-analytic decoding results highlight that changes in region-specific fiber length distribution reflect dynamic adjustments at this stage, potentially contributing to the maturation of key cognitive abilities.

5. Limitation

This study presents several limitations. First, the single-site longitudinal design with a limited sample size suggests the need for larger sample sizes to better delineate regional length changes in the developmental process. Second, the impact of changes in long- and short-range connections across different age periods remains unknown. Future studies should include more data spanning the entire lifespan to assess the proposed metrics as potential biomarkers. Lastly, although we observed overall similar patterns across different brain regions in the simulation tests, the specific differences in geometry-related topological properties among regions and the underlying factors contributing to these regional differences remain unclear. We propose that understanding how change in fiber length median affect topological properties across regions is important and could serve as an intriguing nodal index, reflecting the extent to which geometric constraints influence connectivity. Further research is needed to comprehensively investigate these regional variations. Nevertheless, the consistent topological effect induced by geometry observed in our simulations supports the rationale for using the length median as a nodal metric to characterize network topology.

6. Conclusions

This longitudinal study offers important insights into how brain networks reconfigure during early school age. Our findings suggest that pruning unnecessary long-range connections and increasing short-range connections work together to facilitate network segregation and integration. This dual process reflect the brain's strategy to optimize efficiency by balancing the wiring cost and topological value. These mechanisms are crucial for the hierarchical organization of brain networks and play a pivotal role in cognitive development during early school age. Overall, the study contributes to a deeper understanding of how structural changes in the brain support the cognitive development and adaptation to environmental demands during this crucial developmental stage.

Availability statement

The data and code that support the findings of this study will be made available on request.

CRediT authorship contribution statement

Yanlin Yu: Writing – review & editing, Writing – original draft, Visualization, Validation, Methodology, Investigation, Formal analysis, Data curation, Conceptualization. **Qing Cai:** Writing – review & editing, Supervision, Resources, Project administration, Funding acquisition. **Longnian Lin:** Resources, Project administration, Funding acquisition. **Chu-Chung Huang:** Writing – review & editing, Supervision, Methodology, Investigation, Conceptualization.

Declaration of competing interest

The authors declare that they have no known competing financial interests or personal relationships that could have appeared to influence the work reported in this paper.

Acknowledgments

The authors would like to acknowledge Dr. Chun-Hung Yeh for his valuable discussions on the methodology of this work. This work was funded by Scientific and Technological Innovation 2030 - the major project of the Brain Science and Brain-Inspired Intelligence Technology (2021ZD0200500) and Science and Technology Commission of Shanghai Municipality (19JC1410100).

Supplementary materials

Supplementary material associated with this article can be found, in the online version, at doi:10.1016/j.neuroimage.2025.121066.

Data availability

The data that support the findings of this study will be made available on request.

References

Alexander-Bloch, A.F., Vértes, P.E., Stidd, R., Lalonde, F., Clasen, L., Rapoport, J., Giedd, J., Bullmore, E.T., Gogtay, N., 2013. The anatomical distance of functional connections predicts brain network topology in health and schizophrenia. Cereb. Cortex 23 (1), 127–138. https://doi.org/10.1093/cercor/bhr388.

Assaf, Y., Bouznach, A., Zomet, O., Marom, A., Yovel, Y., 2020. Conservation of brain connectivity and wiring across the mammalian class. Nat. Neurosci. 23 (7). https://doi.org/10.1038/s41593-020-0641-7. Article 7.

Avants, B.B., Tustison, N., Johnson, H., 2009. Adv. Normal. Tools (ANTS) 41.

Bajada, C.J., Schreiber, J., Caspers, S., 2019. Fiber length profiling: a novel approach to structural brain organization. Neuroimage 186, 164–173. https://doi.org/10.1016/j.neuroimage.2018.10.070.

Baker, S.T.E., Lubman, D.I., Yücel, M., Allen, N.B., Whittle, S., Fulcher, B.D., Zalesky, A., Fornito, A., 2015. Developmental changes in brain network hub connectivity in late adolescence. J. Neurosci. 35 (24), 9078–9087. https://doi.org/10.1523/JNEUROSCI.5043-14.2015.

Bassett, D.S., Bullmore, E.T., 2017. Small-world brain networks revisited. Neuroscientist 23 (5), 499–516. https://doi.org/10.1177/1073858416667720.

Bauer, P.J., 2015. Development of episodic and autobiographical memory: the importance of remembering forgetting. Dev. Rev. 38, 146–166. https://doi.org/10.1016/j.dr.2015.07.011.

Baum, G.L., Ciric, R., Roalf, D.R., Betzel, R.F., Moore, T.M., Shinohara, R.T., Kahn, A.E., Vandekar, S.N., Rupert, P.E., Quarmley, M., Cook, P.A., Elliott, M.A., Ruparel, K., Gur, R.E., Gur, R.C., Bassett, D.S., Satterthwaite, T.D., 2017. Modular segregation of structural brain networks supports the development of executive function in youth. Curr. Biol. 27 (11), 1561–1572. https://doi.org/10.1016/j.cub.2017.04.051 e8.

Bazinet, V., Hansen, J.Y., Vos de Wael, R., Bernhardt, B.C., van den Heuvel, M.P., Misic, B., 2023. Assortative mixing in micro-architecturally annotated brain connectomes. Nat. Commun. 14 (1). https://doi.org/10.1038/s41467-023-38585-4. Article 1.

Betzel, R.F., Bassett, D.S., 2018. Specificity and robustness of long-distance connections in weighted, interareal connectomes. Proc. Natl. Acad. Sci. 115 (21), E4880–E4889. https://doi.org/10.1073/pnas.1720186115.

Bullmore, E., Sporns, O., 2012. The economy of brain network organization. Nat. Rev. Neurosci. 13 (5). https://doi.org/10.1038/nrn3214. Article 5.

Cao, M., He, Y., Dai, Z., Liao, X., Jeon, T., Ouyang, M., Chalak, L., Bi, Y., Rollins, N., Dong, Q., Huang, H., 2017. Early development of functional network segregation revealed by connectomic analysis of the preterm Human brain. Cereb. Cortex 27 (3), 1949–1963. https://doi.org/10.1093/cercor/bhw038.

Cassady, K., Gagnon, H., Freiburger, E., Lalwani, P., Simmonite, M., Park, D.C., Peltier, S. J., Taylor, S.F., Weissman, D.H., Seidler, R.D., Polk, T.A., 2020. Network segregation varies with neural distinctiveness in sensorimotor cortex. Neuroimage 212, 116663. https://doi.org/10.1016/j.neuroimage.2020.116663.

DeSerisy, M., Ramphal, B., Pagliaccio, D., Raffanello, E., Tau, G., Marsh, R., Posner, J., Margolis, A.E., 2021. Frontoparietal and default mode network connectivity varies with age and intelligence. Dev. Cogn. Neurosci. 48, 100928. https://doi.org/10.1016/j.dcn.2021.100928.

Dhollander, T., Raffelt, D., & Connelly, A. (2016). *Unsupervised 3-tissue response function estimation from single-shell or multi-shell diffusion MR data without a co-registered T1 image*.

Dong, H.-M., Margulies, D.S., Zuo, X.-N., Holmes, A.J., 2021. Shifting gradients of macroscale cortical organization mark the transition from childhood to adolescence. Proc. Natl. Acad. Sci. 118 (28), e2024448118. https://doi.org/10.1073/pnas.2024448118.

Dubois, J., Alison, M., Counsell, S.J., Hertz-Pannier, L., Hüppi, P.S., Benders, M.J.N.L., 2021. MRI of the Neonatal Brain: a review of methodological challenges and neuroscientific advances. J. Magn. Reson. Imaging 53 (5), 1318–1343. https://doi.org/10.1002/jmri.27192.

Dubois, J., Dehaene-Lambertz, G., Kulikova, S., Poupon, C., Hüppi, P.S., Hertz-Pannier, L., 2014. The early development of brain white matter: a review of imaging studies in fetuses, newborns and infants. Neuroscience 276, 48–71. https://doi.org/10.1016/j.neuroscience.2013.12.044.

Dumontheil, I., Houlton, R., Christoff, K., Blakemore, S.-J., 2010. Development of relational reasoning during adolescence. Dev. Sci. 13 (6), F15–F24. https://doi.org/10.1111/j.1467-7687.2010.01014.x.

Fair, D., Dosenbach, N., Church, J., Cohen, A., Brahmbhatt, S., Miezin, F., Barch, D., Raichle, M., Petersen, S., Schlaggar, B., 2007. Development of distinct control networks through segregation and integration. Proc. Natl. Acad. Sci. U.S.A. 104 (33), 13507–13512. https://doi.org/10.1073/pnas.0705843104.

Feng, G., Chen, R., Zhao, R., Li, Y., Ma, L., Wang, Y., Men, W., Gao, J., Tan, S., Cheng, J., He, Y., Qin, S., Dong, Q., Tao, S., Shu, N., 2023. Longitudinal development of the human white matter structural connectome and its association with brain transcriptomic and cellular architecture. Commun. Biol. 6 (1). https://doi.org/10.1038/s42003-023-05647-8. Article 1.

Geib, B.R., Stanley, M.L., Dennis, N.A., Woldorff, M.G., Cabeza, R., 2017. From hippocampus to whole-brain: the role of integrative processing in episodic memory retrieval. Hum. Brain Mapp. 38 (4), 2242–2259. https://doi.org/10.1002/hbm.23518.

Genc, S., Smith, R.E., Malpas, C.B., Anderson, V., Nicholson, J.M., Efron, D., Sciberras, E., Seal, M.L., Silk, T.J., 2018. Development of white matter fibre density and morphology over childhood: a longitudinal fixel-based analysis. Neuroimage 183, 666–676. https://doi.org/10.1016/j.neuroimage.2018.08.043.

Gooch, D., Thompson, P., Nash, H.M., Snowling, M.J., Hulme, C., 2016. The development of executive function and language skills in the early school years. J. Child Psychol. Psychiatry 57 (2), 180–187. https://doi.org/10.1111/jcpp.12458.

Hagmann, P., Cammoun, L., Gigandet, X., Meuli, R., Honey, C.J., Wedeen, V.J., Sporns, O., 2008. Mapping the structural core of Human cerebral cortex. PLoS Biol. 6 (7), e159. https://doi.org/10.1371/journal.pbio.0060159.

Higo, T., Mars, R.B., Boorman, E.D., Buch, E.R., Rushworth, M.F.S., 2011. Distributed and causal influence of frontal operculum in task control. Proc. Natl. Acad. Sci. 108 (10), 4230–4235. https://doi.org/10.1073/pnas.1013361108.

Horvát, S., Gămănuț, R., Ercsey-Ravasz, M., Magrou, L., Gămănuț, B., Essen, D.C.V., Burkhalter, A., Knoblauch, K., Toroczkai, Z., Kennedy, H., 2016. Spatial embedding and wiring cost constrain the functional layout of the cortical network of rodents and primates. PLoS Biol. 14 (7), e1002512. https://doi.org/10.1371/journal.pbio.1002512.

Hsu, C.-C.H., Chong, S.T., Kung, Y.-C., Kuo, K.-T., Huang, C.-C., Lin, C.-P., 2023. Integrated diffusion image operator (iDIO): a pipeline for automated configuration and processing of diffusion MRI data. *Hum. Brain. Mapp., n/a*(n/a). https://doi.org/10.1002/hbm.26239.

Huang, C.-C., Rolls, E.T., Feng, J., Lin, C.-P., 2022. An extended Human Connectome Project multimodal parcellation atlas of the human cortex and subcortical areas. Brain Struct. Function 227 (3), 763–778. https://doi.org/10.1007/s00429-021-02421-6.

Huang, H., Shu, N., Mishra, V., Jeon, T., Chalak, L., Wang, Z.J., Rollins, N., Gong, G., Cheng, H., Peng, Y., Dong, Q., He, Y., 2015. Development of Human brain structural networks through infancy and childhood. Cereb. Cortex 25 (5), 1389–1404. https://doi.org/10.1093/cercor/bht335.

Jeurissen, B., Tournier, J.-D., Dhollander, T., Connelly, A., Sijbers, J., 2014. Multi-tissue constrained spherical deconvolution for improved analysis of multi-shell diffusion MRI data. Neuroimage 103, 411–426. https://doi.org/10.1016/j.neuroimage.2014.07.061.

Kellner, E., Dhital, B., Kiselev, V.G., Reisert, M., 2016. Gibbs-ringing artifact removal based on local subvoxel-shifts. Magn. Reson. Med. 76 (5), 1574–1581. https://doi.org/10.1002/mrm.26054.

Krogsrud, S.K., Fjell, A., Tamnes, C.K., Grydeland, H., Mork, L., Due-Tønnessen, P., Bjørnerud, A., Sampaio-Baptista, C., Andersson, J., Johansen-Berg, H., Walhovd, K., 2016. Changes in white matter microstructure in the developing brain—A longitudinal diffusion tensor imaging study of children from 4 to 11 years of age. Neuroimage. https://doi.org/10.1016/j.neuroimage.2015.09.017.

Lebel, C., Beaulieu, C., 2011. Longitudinal development of Human brain wiring continues from childhood into adulthood. J. Neurosci. 31 (30), 10937–10947. https://doi.org/10.1523/JNEUROSCI.5302-10.2011.

Lebel, C., Gee, M., Camicioli, R., Wieler, M., Martin, W., Beaulieu, C., 2012. Diffusion tensor imaging of white matter tract evolution over the lifespan. Neuroimage 60 (1), 340–352. https://doi.org/10.1016/j.neuroimage.2011.11.094.

Lebel, C., Treit, S., Beaulieu, C., 2019. A review of diffusion MRI of typical white matter development from early childhood to young adulthood. NMR Biomed. 32 (4). https://doi.org/10.1002/nbm.3778.

Liang, X., Sun, L., Liao, X., Lei, T., Xia, M., Duan, D., Zeng, Z., Xu, Z., Men, W., Wang, Y., Tan, S., Gao, J.-H., Qin, S., Tao, S., Dong, Q., Zhao, T., He, Y., 2022. Structural connectome architecture shapes the maturation of cortical morphology from childhood to adolescence. bioRxiv., 520527 https://doi.org/10.1101/2022.12.15.520527.

Low, L.K., Cheng, H.-J., 2006. Axon pruning: an essential step underlying the developmental plasticity of neuronal connections. Philosoph. Trans. R. Soc. B: Biol. Sci. 361 (1473), 1531–1544. https://doi.org/10.1098/rstb.2006.1883.

Marek, S., Hwang, K., Foran, W., Hallquist, M.N., Luna, B., 2015. The contribution of network organization and integration to the development of cognitive control. PLoS Biol. 13 (12), e1002328. https://doi.org/10.1371/journal.pbio.1002328.

Margulies, D.S., Ghosh, S.S., Goulas, A., Falkiewicz, M., Huntenburg, J.M., Langs, G., Bezgin, G., Eickhoff, S.B., Castellanos, F.X., Petrides, M., Jefferies, E., Smallwood, J., 2016. Situating the default-mode network along a principal gradient of macroscale cortical organization. Proc. Natl. Acad. Sci. 113 (44), 12574–12579. https://doi.org/10.1073/pnas.1608282113.

Menon, V., 2013. Developmental pathways to functional brain networks: emerging principles. Trends Cogn. Sci. (Regul. Ed.) 17 (12), 627–640. https://doi.org/10.1016/j.tics.2013.09.015.

Milisav, F., Misic, B., 2023. Spatially embedded neuromorphic networks. Nat. Mach. Intell. 5 (12), 1342–1343. https://doi.org/10.1038/s42256-023-00771-w.

Nagy, Z., Westerberg, H., Klingberg, T., 2004. Maturation of white matter is associated with the development of cognitive functions during childhood. J. Cogn. Neurosci. 16 (7), 1227–1233. https://doi.org/10.1162/0898929041920441.

Oldham, S., Ball, G., Fornito, A., 2022. Early and late development of hub connectivity in the human brain. Curr. Opin. Psychol. 44, 321–329. https://doi.org/10.1016/j.copsyc.2021.10.010.

Oldham, S., Fornito, A, 2019. The development of brain network hubs. Dev. Cogn. Neurosci. 36, 100607. https://doi.org/10.1016/j.dcn.2018.12.005.

Ouyang, M., Kang, H., Detre, J.A., Roberts, T.P.L., Huang, H., 2017. Short-range connections in the developmental connectome during typical and atypical brain maturation. Neurosci. Biobehav. Rev. 83, 109–122. https://doi.org/10.1016/j.neubiorev.2017.10.007.

Oyefiade, A.A., Ameis, S., Lerch, J.P., Rockel, C., Szulc, K.U., Scantlebury, N., Decker, A., Jefferson, J., Spichak, S., Mabbott, D.J., 2018. Development of short-range white

matter in healthy children and adolescents. Hum. Brain Mapp. 39 (1), 204–217. https://doi.org/10.1002/hbm.23836.
Pang, J.C., Aquino, K.M., Oldehinkel, M., Robinson, P.A., Fulcher, B.D., Breakspear, M., Fornito, A., 2023. Geometric constraints on human brain function. Nature 1–9. https://doi.org/10.1038/s41586-023-06098-1.
Paquola, C., Wael, R.V.D., Wagstyl, K., Bethlehem, R.A.I., Hong, S.-J., Seidlitz, J., Bullmore, E.T., Evans, A.C., Misic, B., Margulies, D.S., Smallwood, J., Bernhardt, B. C., 2019. Microstructural and functional gradients are increasingly dissociated in transmodal cortices. PLoS Biol. 17 (5), e3000284. https://doi.org/10.1371/journal.pbio.3000284.
Neuroscience in Psychiatry Network (NSPN) Consortium Park, B., Paquola, C., Bethlehem, R.A.I., Benkarim, O., 2022. Adolescent development of multiscale structural wiring and functional interactions in the human connectome. In: Mišić, B., Smallwood, J., Bullmore, E.T., Bernhardt, B.C. (Eds.), 119, e2116673119. https://doi.org/10.1073/pnas.2116673119.
Parlatini, V., Radua, J., Dell'Acqua, F., Leslie, A., Simmons, A., Murphy, D.G., Catani, M., Thiebaut de Schotten, M., 2017. Functional segregation and integration within fronto-parietal networks. Neuroimage 146, 367–375. https://doi.org/10.1016/j.neuroimage.2016.08.031.
Patenaude, B., Smith, S.M., Kennedy, D.N., Jenkinson, M., 2011. A Bayesian model of shape and appearance for subcortical brain segmentation. Neuroimage 56 (3), 907–922. https://doi.org/10.1016/j.neuroimage.2011.02.046.
Peters, B.D., Ikuta, T., DeRosse, P., John, M., Burdick, K.E., Gruner, P., Prendergast, D.M., Szeszko, P.R., Malhotra, A.K., 2014. Age-related differences in white matter tract microstructure are associated with cognitive performance from childhood to adulthood. Biol. Psychiatry 75 (3), 248–256. https://doi.org/10.1016/j.biopsych.2013.05.020.
Puxeddu, M.G., Faskowitz, J., Betzel, R.F., Petti, M., Astolfi, L., Sporns, O., 2020. The modular organization of brain cortical connectivity across the human lifespan. Neuroimage 218, 116974. https://doi.org/10.1016/j.neuroimage.2020.116974.
Raffelt, D., Dhollander, T., Tournier, J.-D., Tabbara, R., Smith, R., Pierre, E., & Connelly, A. (2017). *Bias Field Correction and Intensity Normalisation for Quantitative Analysis of Apparent Fibre Density*.
Rankin, J., Rinzel, J., 2019. Computational models of auditory perception from feature extraction to stream segregation and behavior. Curr. Opin. Neurobiol. 58, 46–53. https://doi.org/10.1016/j.conb.2019.06.009.
Razban, R.M., Pachter, J.A., Dill, K.A., Mujica-Parodi, L.R., 2023. Early path dominance as a principle for neurodevelopment. Proc. Natl. Acad. Sci. 120 (16), e2218007120. https://doi.org/10.1073/pnas.2218007120.
Rubinov, M., Sporns, O., 2010. Complex network measures of brain connectivity: uses and interpretations. Neuroimage 52 (3), 1059–1069. https://doi.org/10.1016/j.neuroimage.2009.10.003.
Sepulcre, J., Liu, H., Talukdar, T., Martincorena, I., Yeo, B., Buckner, R., 2010. The organization of local and distant functional connectivity in the Human brain. PLoS Comput. Biol. 6 (6). https://doi.org/10.1371/journal.pcbi.1000808.
Sherman, L.E., Rudie, J.D., Pfeifer, J.H., Masten, C.L., McNealy, K., Dapretto, M., 2014. Development of the default mode and Central executive networks across early adolescence: a longitudinal study. Dev. Cogn. Neurosci. 10, 148–159. https://doi.org/10.1016/j.dcn.2014.08.002.
Smallwood, J., Bernhardt, B.C., Leech, R., Bzdok, D., Jefferies, E., Margulies, D.S., 2021. The default mode network in cognition: a topographical perspective. Nat. Rev. Neurosci. 22 (8). https://doi.org/10.1038/s41583-021-00474-4. Article 8.
Smith, R.E., Tournier, J.-D., Calamante, F., Connelly, A., 2012. Anatomically-constrained tractography: improved diffusion MRI streamlines tractography through effective use of anatomical information. Neuroimage 62 (3), 1924–1938. https://doi.org/10.1016/j.neuroimage.2012.06.005.
Smith, R.E., Tournier, J.-D., Calamante, F., Connelly, A., 2013. SIFT: spherical-deconvolution informed filtering of tractograms. Neuroimage 67, 298–312. https://doi.org/10.1016/j.neuroimage.2012.11.049.
Smith, R.E., Tournier, J.-D., Calamante, F., Connelly, A., 2015a. SIFT2: enabling dense quantitative assessment of brain white matter connectivity using streamlines tractography. Neuroimage 119, 338–351. https://doi.org/10.1016/j.neuroimage.2015.06.092.
Smith, R.E., Tournier, J.-D., Calamante, F., Connelly, A., 2015b. The effects of SIFT on the reproducibility and biological accuracy of the structural connectome. Neuroimage 104, 253–265. https://doi.org/10.1016/j.neuroimage.2014.10.004.
Smith, S.M., 2002. Fast robust automated brain extraction. Hum. Brain Mapp. 17 (3), 143–155. https://doi.org/10.1002/hbm.10062.
Smith, S.M., Jenkinson, M., Woolrich, M.W., Beckmann, C.F., Behrens, T.E.J., Johansen-Berg, H., Bannister, P.R., De Luca, M., Drobnjak, I., Flitney, D.E., Niazy, R.K., Saunders, J., Vickers, J., Zhang, Y., De Stefano, N., Brady, J.M., Matthews, P.M., 2004. Advances in functional and structural MR image analysis and implementation as FSL. Neuroimage 23, S208–S219. https://doi.org/10.1016/j.neuroimage.2004.07.051.
Snyder, J.S., Alain, C., 2007. Toward a neurophysiological theory of auditory stream segregation. Psychol. Bull. 133 (5), 780–799. https://doi.org/10.1037/0033-2909.133.5.780.
Sporns, O., Honey, C.J., 2006. Small worlds inside big brains. Proc. Natl. Acad. Sci. 103 (51), 19219–19220. https://doi.org/10.1073/pnas.0609523103.
Sporns, O., Honey, C.J., Kotter, R., 2007. Identification and classification of hubs in brain networks. PLoS. One 2 (10). https://doi.org/10.1371/journal.pone.0001049.
Sporns, O., Zwi, J.D., 2004. The small world of the cerebral cortex. Neuroinformatics 2 (2), 145–162. https://doi.org/10.1385/NI:2:2:145.
Stikov, N., Perry, L.M., Mezer, A., Rykhlevskaia, E., Wandell, B.A., Pauly, J.M., Dougherty, R.F., 2011. Bound pool fractions complement diffusion measures to describe white matter micro and macrostructure. Neuroimage 54 (2), 1112–1121. https://doi.org/10.1016/j.neuroimage.2010.08.068.
Strong, W.B., Malina, R.M., Blimkie, C.J.R., Daniels, S.R., Dishman, R.K., Gutin, B., Hergenroeder, A.C., Must, A., Nixon, P.A., Pivarnik, J.M., Rowland, T., Trost, S., Trudeau, F., 2005. Evidence based physical activity for school-age youth. J. Pediatr. 146 (6), 732–737. https://doi.org/10.1016/j.jpeds.2005.01.055.
Thiebaut de Schotten, M., Forkel, S.J., 2022. The emergent properties of the connected brain. Science (1979) 378 (6619), 505–510. https://doi.org/10.1126/science.abq2591.
Tooley, U.A., Park, A.T., Leonard, J.A., Boroshok, A.L., McDermott, C.L., Tisdall, M.D., Bassett, D.S., Mackey, A.P., 2022. The age of reason: functional brain network development during childhood. J. Neuroscience 42 (44), 8237–8251. https://doi.org/10.1523/JNEUROSCI.0511-22.2022.
Tournier, J.-D., Calamante, F., Connelly, A., 2010. Improved probabilistic streamlines tractography by 2nd order integration over fibre orientation distributions. In: Proceedings of the International Society for Magnetic Resonance in Medicine, p. 1.
Tustison, N.J., Avants, B.B., Cook, P.A., Zheng, Y., Egan, A., Yushkevich, P.A., Gee, J.C., 2010. N4ITK: improved N3 bias correction. IEEe Trans. Med. ImAging 29 (6), 1310–1320. https://doi.org/10.1109/TMI.2010.2046908. IEEE Transactions on Medical Imaging.
Veraart, J., Novikov, D.S., Christiaens, D., Ades-aron, B., Sijbers, J., Fieremans, E., 2016. Denoising of diffusion MRI using random matrix theory. Neuroimage 142, 394–406. https://doi.org/10.1016/j.neuroimage.2016.08.016.
Vos, S.B., Tax, C.M.W., Luijten, P.R., Ourselin, S., Leemans, A., Froeling, M., 2017. The importance of correcting for signal drift in diffusion MRI. Magn. Reson. Med. 77 (1), 285–299. https://doi.org/10.1002/mrm.26124.
Wang, C., Hu, Y., Weng, J., Chen, F., Liu, H., 2020. Modular segregation of task-dependent brain networks contributes to the development of executive function in children. Neuroimage 206, 116334. https://doi.org/10.1016/j.neuroimage.2019.116334.
Westphal, A.J., Wang, S., Rissman, J., 2017. Episodic memory retrieval benefits from a less modular brain network organization. J. Neurosci. 37 (13), 3523–3531. https://doi.org/10.1523/JNEUROSCI.2509-16.2017.
Wu, K., Taki, Y., Sato, K., Hashizume, H., Sassa, Y., Takeuchi, H., Thyreau, B., He, Y., Evans, A.C., Li, X., Kawashima, R., Fukuda, H., 2013. Topological organization of functional brain networks in healthy children: differences in relation to age, sex, and intelligence. PLoS. One 8 (2), e55347. https://doi.org/10.1371/journal.pone.0055347.
Xia, Y., Xia, M., Liu, J., Liao, X., Lei, T., Liang, X., Zhao, T., Shi, Z., Sun, L., Chen, X., Men, W., Wang, Y., Pan, Z., Luo, J., Peng, S., Chen, M., Hao, L., Tan, S., Gao, J.-H., He, Y., 2022. Development of functional connectome gradients during childhood and adolescence. Sci. Bull. (Beijing) 67 (10), 1049–1061. https://doi.org/10.1016/j.scib.2022.01.002.
Yarkoni, T., Poldrack, R.A., Nichols, T.E., Van Essen, D.C., Wager, T.D., 2011. Large-scale automated synthesis of human functional neuroimaging data. Nat. Methods 8 (8). https://doi.org/10.1038/nmeth.1635. Article 8.
Yu, Q., Peng, Y., Kang, H., Peng, Q., Ouyang, M., Slinger, M., Hu, D., Shou, H., Fang, F., Huang, H., 2020. Differential white matter maturation from birth to 8 years of age. Cereb. Cortex 30 (4), 2674–2690. https://doi.org/10.1093/cercor/bhz268.
Zhao, T., Cao, M., Niu, H., Zuo, X.-N., Evans, A., He, Y., Dong, Q., Shu, N., 2015. Age-related changes in the topological organization of the white matter structural connectome across the human lifespan. Hum. Brain Mapp. 36 (10), 3777–3792. https://doi.org/10.1002/hbm.22877.
Zhao, T., Mishra, V., Jeon, T., Ouyang, M., Peng, Q., Chalak, L., Wisnowski, J.L., Heyne, R., Rollins, N., Shu, N., Huang, H., 2019. Structural network maturation of the preterm human brain. Neuroimage 185, 699–710. https://doi.org/10.1016/j.neuroimage.2018.06.047.